

Infrared and Visible Absorption Spectra of Doped $(\text{CH})_x$, $(\text{CD})_x$, and Copolymers $[(\text{C}_2\text{H}_2)_{1-y}(\text{C}_2\text{D}_2)_y]_x$

Hitoshi FUJIMOTO, Masashi TANAKA,*† and Jiro TANAKA

Department of Chemistry, Faculty of Science, Nagoya University, Chikusa-ku, Nagoya 464

†Department of Chemistry, College of General Education, Nagoya University, Chikusa-ku, Nagoya 464

(Received June 17, 1982)

Infrared and visible absorption spectra of $(\text{CH})_x$, $(\text{CD})_x$, and the copolymers $[(\text{C}_2\text{H}_2)_{1-y}(\text{C}_2\text{D}_2)_y]_x$ doped with Br_2 or I_2 were measured for various values of y between 0 and 1. By the doping, the $\pi \rightarrow \pi^*$ band located in the 19000 cm^{-1} region disappeared while several new bands were observed at $800\text{--}900\text{--}$, $1000\text{--}1400\text{--}$, and 5000--cm^{-1} regions. The absorption band shapes and the locations of the 5000-- and 19000--cm^{-1} bands did not depend appreciably upon the value of y . The charged soliton induced vibrational bands were found at 870-- and 1370--cm^{-1} in $(\text{CH})_x$ and 1230-- , 1100-- , and 780--cm^{-1} in $(\text{CD})_x$. In addition, another new bands were found around $570\text{--}660\text{ cm}^{-1}$ region by decreasing the temperature of the doped film to 160 K . These new bands were not shifted by the isotopic substitution. A plausible mechanism for the appearance of this band is suggested as an oscillation of trapped charged soliton around the negatively charged dopant. For the heavily doped $(\text{CH})_x$ film, the gapless transition was observed and the optical conductivity was estimated by the Drude formula and was compared with the value obtained by a direct conductivity measurement.

Polyacetylene, $(\text{CH})_x$, is one of the simplest linear conjugated polymers with a single chain structure and is a large band gap semiconductor. That is, pure $(\text{CH})_x$ has the configuration of alternating single and double bonds and the $\pi \rightarrow \pi^*$ transition at about 19000 cm^{-1} indicates that the band gap exists due to the bond alternation in the polymer. However, Shirakawa, Heeger, and MacDiarmid and coworkers^{1,2)} found that this polymer undergoes dramatic increase in electrical conductivity upon exposure to vapors of chlorine, bromine, iodine, and arsenic pentafluoride. Furthermore, doping changes the color of thin films from reddish cupric to transparent blue. Such color change occurs by a new absorption band which may be due to charged soliton or free carrier and the suppression of the $\pi \rightarrow \pi^*$ interband transition. Many optical^{3–7} and theoretical^{8–10)} studies have been presented hitherto to study the above-mentioned spectral changes, but the studies on the charged soliton state are not yet established. For instance, the new bands specific to the doped $(\text{CH})_x$ are observed around 1370-- , 1280-- , and 870--cm^{-1} .^{11–14)} Doped $(\text{CD})_x$ films also show additional bands which are located at 1230-- , 1100-- , and 780--cm^{-1} . These additional bands were assigned to the charged soliton-induced infrared absorption bands.^{15–17)} On the other hand Raman studies on $(\text{CH})_x$ and $(\text{CD})_x$ indicated that the bond alternation still remained or even enhanced after doping,¹⁸⁾ and ^{13}C NMR measurement did not show presence of Knight shift.¹⁹⁾

In the present paper, we report the optical absorption spectra of Br_2 or I_2 doped $(\text{CH})_x$, $(\text{CD})_x$, and copolymers $[(\text{C}_2\text{H}_2)_{1-y}(\text{C}_2\text{D}_2)_y]_x$ and discuss the change of spectra with varying the y of deuterium composition. The temperature effect upon the $500\text{--}800\text{ cm}^{-1}$ band of these films was studied, and new bands were found just as were found in our earlier paper on the AsF_5 or Br_2 doped $(\text{CH})_x$.⁷⁾

Experimental

The copolymer films, $[(\text{C}_2\text{H}_2)_{1-y}(\text{C}_2\text{D}_2)_y]_x$, were prepared from the mixture of acetylene and acetylene- d_2 gases by Shirakawa's method.²⁰⁾ Acetylene was purified before use

by being passed successively through a concentrated sulfuric acid solution and Dry Ice-acetone traps. Acetylene- d_2 was prepared by adding heavy water to calcium carbide under vacuum. The isotopic contents were determined by partial pressure of C_2H_2 and C_2D_2 .

The thin film was polymerized on the teflon frame with a $4 \times 8\text{ mm}^2$ hole and mounted in the Dewar vessel. Doping was accomplished by exposure of the film mounted in the Dewar vessel to bromine or iodine vapor. The extent of doping was controlled by measuring the four-probe d.c. conductivity of another thick film. After doping, the film was pumped out for at least 30 min and the infrared absorption of the film was measured with a Hitachi IR 260-50 ($350\text{--}4000\text{ cm}^{-1}$). Low temperature measurements were made by putting a liquid nitrogen into the Dewar vessel (see Fig. 1). For the visible absorption measurement, the thin film was polymerized on the inner surface of the 1 cm quartz cell and the absorption spectra of the films were measured with a Carl-Zeiss spectrophotometer ($4000\text{--}45000\text{ cm}^{-1}$) after doping.

The best fit of the calculated absorption spectrum to the observed spectrum of Br_2 doped $(\text{CH})_x$ film was made on a FACOM M-200 computer of Nagoya University by using the SALS program.

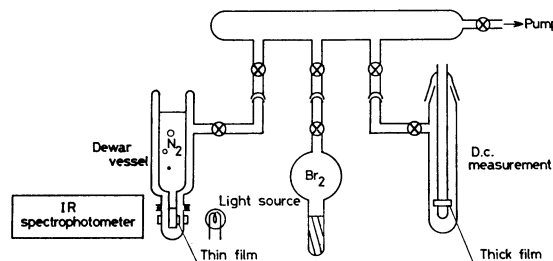


Fig. 1. Apparatus of the system of doping and IR absorption measurement.

Results and Discussion

Absorption Spectra of Thin $(\text{CH})_x$ Films Doped with Br_2 . Pure $(\text{CH})_x$ film has a strong $\pi \rightarrow \pi^*$ band in the 19000 cm^{-1} region besides the C–H out-of-plane

(740 cm^{-1} in *cis*- $(\text{CH})_x$ and 1015 cm^{-1} in *trans*- $(\text{CH})_x$) and the C–C–C deformation (446 cm^{-1} in *cis*- $(\text{CH})_x$). Figures 2 and 3 show the change of spectra by doping:

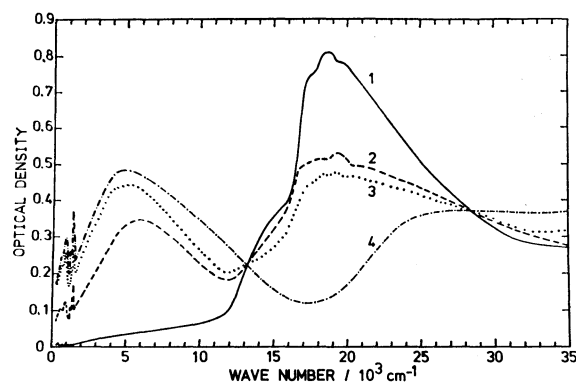


Fig. 2. Absorption spectra of the thin $(\text{CH})_x$ films doped with Br_2 .

1: Pure, 2: $\sigma \approx 6 \Omega^{-1} \text{cm}^{-1}$, 3: $\sigma \approx 30 \Omega^{-1} \text{cm}^{-1}$, 4: $\sigma \approx 40 \Omega^{-1} \text{cm}^{-1}$.

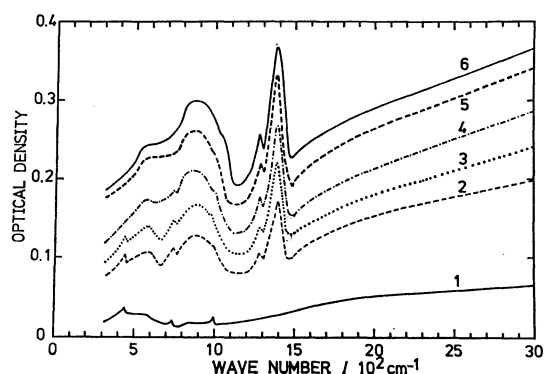


Fig. 3. IR absorption spectra of the thin $(\text{CH})_x$ films doped with Br_2 .

1: pure, 2: $\sigma \approx 1 \Omega^{-1} \text{cm}^{-1}$, 3: $\sigma \approx 6 \Omega^{-1} \text{cm}^{-1}$, 4: $\sigma \approx 15 \Omega^{-1} \text{cm}^{-1}$, 5: $\sigma \approx 30 \Omega^{-1} \text{cm}^{-1}$, 6: $\sigma \approx 40 \Omega^{-1} \text{cm}^{-1}$.

a new broad absorption band is observed over the wide region from 300- to 25000- cm^{-1} , while the $\pi \rightarrow \pi^*$ band at 19000 cm^{-1} is diminished and the absorption band of the Br_3^- ion appears in the 23000–35000 cm^{-1} region. Several new vibrational peaks are found at 1370-, 1280-, and 870- cm^{-1} , two of which were assigned by Mele and Rice¹⁵⁾ as the charged soliton-induced vibrations of C–C, C=C, and C–H bonds. Furthermore, the 1015 cm^{-1} band, which is the C–H out-of-plane band of *trans*-($\text{CH})_x$, is intensified although the 740- and 446- cm^{-1} bands assigned to the vibrational bands of *cis*-($\text{CH})_x$ are disappeared. This fact means that the doping induces the *cis-trans* isomerization of the $(\text{CH})_x$ films.

Analysis of the Free Carrier Like Absorption Band of Heavily Br_2 Doped $(\text{CH})_x$ Film.

The observed optical density of thin films includes the contribution of the multiple reflection from the sample surface. Then, the absorption coefficient is determined from the observed transmittance as follows,²¹⁾

$$T = \frac{(1-R)^2 e^{-\alpha d}}{1-R^2 e^{-2\alpha d}}, \quad (1)$$

where T is the observed transmittance, α the absorption coefficient, d the sample thickness, and R the surface reflectivity. Accordingly, the absorption coefficient is given by the following equation,

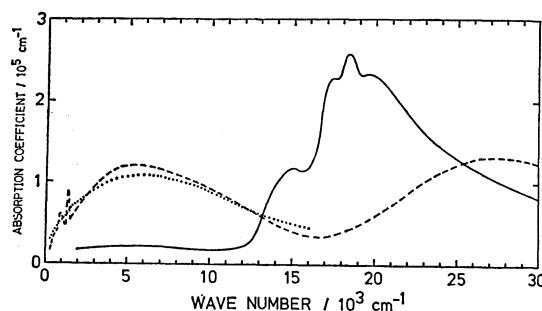


Fig. 4. Absorption spectra of pure and Br_2 doped $(\text{CH})_x$.

—: Pure, ----: observed spectra of doped $(\text{CH})_x$,: calculated spectra of doped $(\text{CH})_x$.

$$\alpha = \frac{1}{d} \ln \left\{ \frac{(1-R)^2}{2T} + \left[\frac{(1-R)^4}{4T^2} + R^2 \right]^{1/2} \right\}. \quad (2)$$

As the surface reflectivity R corresponds to the measured reflectivity of the thick $(\text{CH})_x$ film, the absorption spectra of pure and Br_2 doped thin $(\text{CH})_x$ films are estimated as is shown in Fig. 4. Here, the thickness, d , of the film is determined by equating the maximum absorption coefficient of the 19000 cm^{-1} band to $2.58 \times 10^5 \text{cm}^{-1}$.⁵⁾ This value was determined by K-K transformations of the reflection spectra of pure thick films.

The absorption coefficient of the film, $\alpha(\omega)$, is expressed by using the complex dielectric constant, $\epsilon(\omega)$, as follows,⁵⁾

$$\alpha(\omega) = \frac{\sqrt{2}\omega}{c} \{ (\epsilon_1^2 + \epsilon_2^2)^{1/2} - \epsilon_1 \}^{1/2}, \quad (3)$$

and,

$$\epsilon(\omega) = \epsilon_1(\omega) + i\epsilon_2(\omega). \quad (4)$$

In the heavily doped $(\text{CH})_x$ film, the 19000 cm^{-1} band corresponding to the interband transition disappears in the visible region and the broad band appears in the IR region having maximum at about 5500 cm^{-1} . The edge of the broad absorption band is not clearly found because of the overlapping with vibrational and soliton-induced bands. However, it seems to be decreasing less than 300 cm^{-1} with increasing doping, therefore the band gap seems to be closing at the final stage of doping.

Accordingly, if we suppose that the free carrier is formed by the heavy doping, then the complex dielectric constant will be given by a Drude type equation as,

$$\epsilon(\omega) = \epsilon_{\text{core}} - \frac{\omega_p^2}{\omega^2 + i\gamma\omega} \quad (5)$$

$$\epsilon_1(\omega) = \epsilon_{\text{core}} - \frac{\omega_p^2}{\omega^2 + \gamma^2}, \quad (6)$$

and,

$$\epsilon_2(\omega) = \frac{\gamma}{\omega} \frac{\omega_p^2}{\omega^2 + \gamma^2}, \quad (7)$$

where ω_p is the plasma frequency and γ the band width.

For the heavily Br_2 doped $(\text{CH})_x$ film, the parameters of Eqs. 6 and 7 are determined by the optimum fit of Eq. 3 to the experimental data of Eq. 2. The

best fit is obtained with $\hbar\omega_p=18200\text{ cm}^{-1}$, $\gamma=8270\text{ cm}^{-1}$, and $\epsilon_{\text{core}}=2.77$. The calculated absorption spectrum based on these values is plotted for comparison with the experimental curve in Fig. 4. If we assume that the effective mass of the free carrier is equal to the electron mass, then the number of density, N , of the free carrier contributing to the metallic conduction is given as follows,

$$N = \frac{\omega_p^2 m_e}{4\pi e^2}. \quad (8)$$

Accordingly, the density of free carrier in the heavily doped $(\text{CH})_x$ film is estimated as $3.0 \times 10^{21}\text{ cm}^{-3}$. The total number of π -electron per unit volume was considered as $1.8 \times 10^{22}\text{ cm}^{-3}$ from the specific gravity 0.4 g/cm^3 of $(\text{CH})_x$ film.³⁾ Therefore, one-sixth of all π -electrons are considered to be susceptible to the optical excitation of gapless transition.

By using the values of ω_p and γ , the conductivity of the doped film shown in Fig. 4 is estimated as being $67\text{ }\Omega^{-1}\text{ cm}^{-1}$. The measured value was $40\text{ }\Omega^{-1}\text{ cm}^{-1}$; the agreement is reasonably good. The content of the dopant determined by chemical analysis was correlated with the conductivity, and the present heavily doped film includes 4% of tribromide ion (Br_3^-) per carbon atom. Therefore, one positive carbon atom or charged soliton may exist for twenty-five neutral atoms on an average. Since the probability density of the charged soliton spreads around the positive center, it is remarked that the π -electrons around the charged soliton may be responsible for the gapless transition.

Under the condition that the bond alternation exists in the chain, several mechanisms may be possible for the appearance of the gapless transition. One of them is based on the excitation of electrons around the positively charged soliton. Mele and Rice⁶⁾ have calculated the band structure of midgap state showing that the semiconductor to metal transition may occur by the heavy doping.

Absorption Spectra of Thin $(\text{CD})_x$ Films Doped with Br_2 . The spectra of the thin *cis*- $(\text{CD})_x$ film are shown in Fig. 5, and the overall spectral change with Br_2 doping is illustrated in the order of increasing dopant concentration. The spectra observed in the

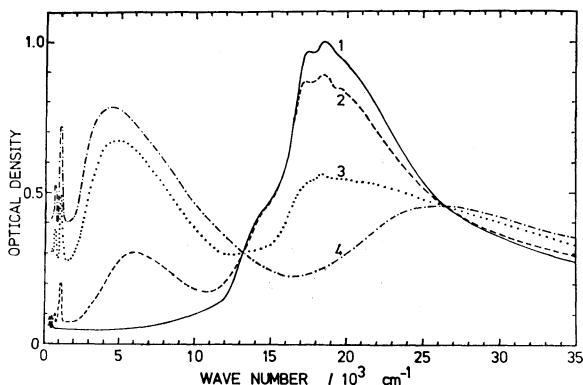


Fig. 5. Absorption spectra of the thin $(\text{CD})_x$ films doped with Br_2 .
1: Pure, 2: $\sigma \approx 0.1\text{ }\Omega^{-1}\text{ cm}^{-1}$, 3: $\sigma \approx 2\text{ }\Omega^{-1}\text{ cm}^{-1}$, 4: $\sigma \approx 4\text{ }\Omega^{-1}\text{ cm}^{-1}$.

near IR to visible region are similar to those of pure and Br_2 doped $(\text{CH})_x$. That is, the strong peak around 19000 cm^{-1} , which is the $\pi \rightarrow \pi^*$ transition of the *cis* form, disappears and intense band grows up at 6000 cm^{-1} as a peak and its maximum moves to 4600 cm^{-1} at the final stage of doping. The position of the peak maxima shifts slightly to red by 200 cm^{-1} in $(\text{CD})_x$ as compared to $(\text{CH})_x$.

In Fig. 6 the spectral change in the IR region is shown with expanded scale. The tail of the 4600 cm^{-1} absorption band falls down gradually and it is overlapped with vibrational bands in the lower energy region. For the heavily doped film the low frequency part is enhanced and it appears to show an onset of the gapless transition. The new bands are observed at 1100- and 770-cm^{-1} regions with Br_2 doping. These bands are correlated with the 1370- and 870-cm^{-1} bands in $(\text{CH})_x$, and the positions and the intensities of these bands are in excellent agreement with the calculation of Mele¹⁶⁾ and Etemad *et al.*¹⁷⁾ as shown in Fig. 6. This result is in conformity with Etemad's result, but our spectra show a shoulder at 1230 cm^{-1} which was predicted at 1270 cm^{-1} and was not clearly indicated in the earlier study.¹⁷⁾

Temperature Dependence of Br_2 and I_2 Doped Thin Films. The changes of IR bands with temperature are measured in $160\text{--}300\text{ K}$ with Br_2 doped $(\text{CD})_x$ and $(\text{CH})_x$

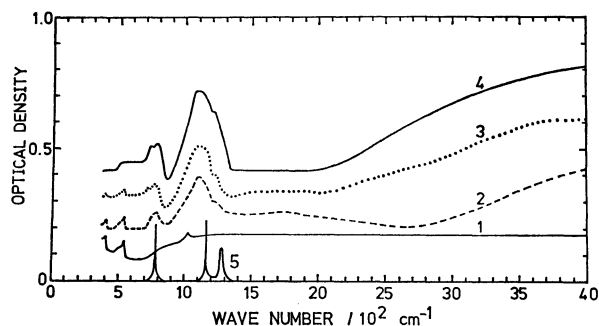


Fig. 6. IR absorption spectra of the thin $(\text{CD})_x$ films doped with Br_2 .

1: Pure, 2: $\sigma \approx 0.1\text{ }\Omega^{-1}\text{ cm}^{-1}$, 3: $\sigma \approx 1.3\text{ }\Omega^{-1}\text{ cm}^{-1}$, 4: $\sigma \approx 4\text{ }\Omega^{-1}\text{ cm}^{-1}$, 5: calculated by Mele and Rice.¹⁶⁾

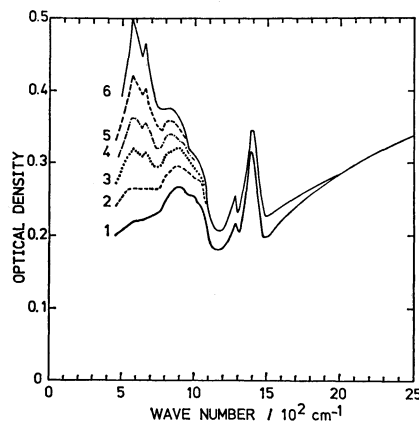


Fig. 7. Temperature dependence of the IR absorption spectra of the heavily Br_2 doped thin $(\text{CH})_x$ film.
1: 300 K , 2: 280 K , 3: 260 K , 4: 230 K , 5: 200 K , 6: 140 K .

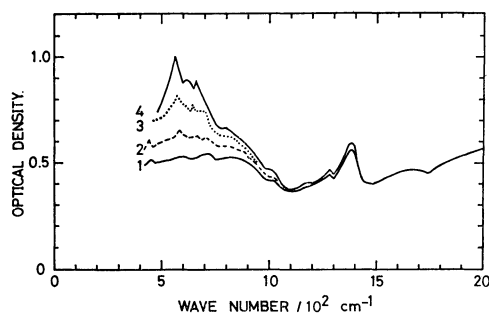


Fig. 8. Temperature dependence of the IR absorption spectra of the heavily I_2 doped thin $(CH)_x$ film. 1: 300 K, 2: 270 K, 3: 240 K, 4: 230 K.

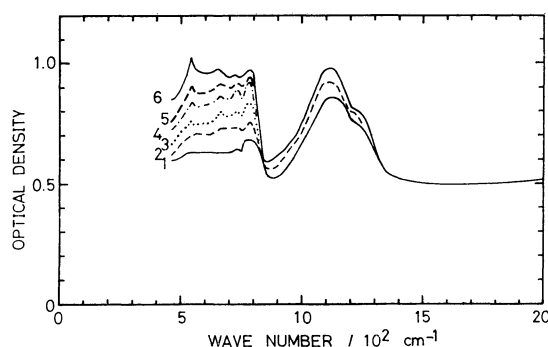


Fig. 9. Temperature dependence of the IR absorption spectra of the heavily Br_2 doped thin $(CD)_x$ film. 1: 300 K, 2: 280 K, 3: 260 K, 4: 240 K, 5: 220 K, 6: 160 K.

and I_2 doped $(CH)_x$. The spectral changes are illustrated in Figs. 7, 8, and 9. A common feature of spectral change is an appearance of new bands around 600 cm^{-1} region. It is remarkable that similar strong bands are observed with these films in spite of differences in isotopic species or chemical dopants. It should be remarked that the AsF_5 doped film showed the same spectral change in this region.⁷⁾

In Fig. 7, the lower frequency bands around $400\text{--}1000\text{ cm}^{-1}$ are shown to be enhanced by cooling, and new peaks appear at 570-- and 660 cm^{-1} . The 1370 cm^{-1} band and the broad absorption above 2000 cm^{-1} are not enhanced appreciably for this temperature range. In Fig. 8, the spectral change of the I_2 doped $(CH)_x$ film is illustrated, and the same peaks are found at 570-- and 660 cm^{-1} . The Br_2 doped $(CD)_x$ film showed remarkably parallel spectral change by lowering the temperature; the broad bands around $500\text{--}800\text{ cm}^{-1}$ are enhanced and new peaks are found at 540-- and 660 cm^{-1} . The deuterium substitution influences the new band as being found at slightly lower frequency. Moreover the skeletal vibration around 800 cm^{-1} is overlapped with new bands.

As regard to the origin of the new band, the predictions given by Mele and Rice¹⁵⁾ and Su, Schrieffer, and Heeger²²⁾ on the soliton pinning mode should be mentioned. Mele and Rice¹⁵⁾ inferred that the far-infrared absorption may be found around $300\text{--}500\text{ cm}^{-1}$ by the pinning of the charged soliton, but they did not mention on the temperature effect on the soliton motion. Su, Schrieffer, and Heeger²²⁾ have

shown the pinning modes to appear at 560-- and 720 cm^{-1} , and the lower one is due to the bound state of the charged soliton with the dopant and the higher one is a length or shape oscillation. The observed band positions are in excellent agreement with their calculations, but the assignment of the mode is difficult. The absence of isotopic effect indicates that the transition is essentially an electronic or the charged soliton's origin. The independence of the band position on the dopant species also support the soliton mechanism, because an impurity trapped bound state in the semiconductor is sensitive to acceptor species.²³⁾

The observed intensities of new bands are exceeding as compared to usual vibrational band. We have estimated the transition moment of the pinning mode of the charged soliton by a harmonic oscillator model with parameters given by Su, Schrieffer, and Heeger,²²⁾ and the value was reasonable with their soliton mass of $6 m_e$.

The absence of pinning mode at room temperature may be understood by the rapid motion of the charged soliton, because the energy of the pinning mode is dependent on the distance between the positively charged soliton and the dopant anion, and it might be smeared out at high temperature by the rapid motion. With decreasing the temperature, the charged soliton might be trapped at the proximity of anion, and the oscillatory motion will start around the anion.

IR Absorption Spectra of Thin Copolymers $[(C_2H_2)_{1-y}-(C_2D_2)_y]_x$ Doped with Br_2 . In Fig. 10, the room temperature and low temperature absorption spectra of copolymers are shown for the following compositions: $y=0, 0.2, 0.5, 0.8$, and 1.0 . The 870 cm^{-1} band in the Br_2 doped $(CH)_x$ ($y=0$) shifts to lower frequencies with increasing y . A more careful examination

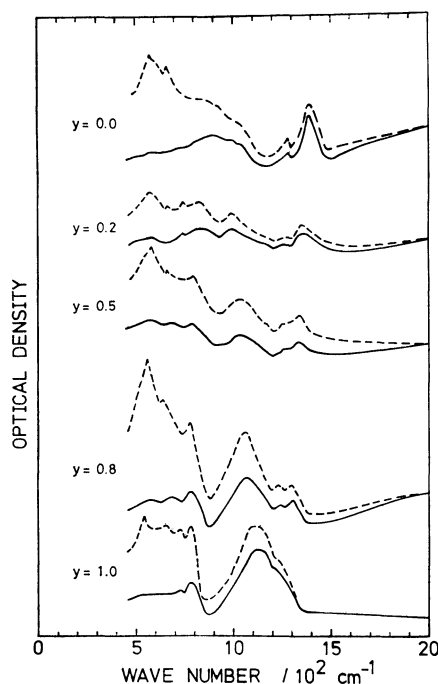


Fig. 10. IR absorption spectra of copolymers $[(C_2H_2)_{1-y}-(C_2D_2)_y]_x$ doped with Br_2 . —: 300 K,: 160 K.

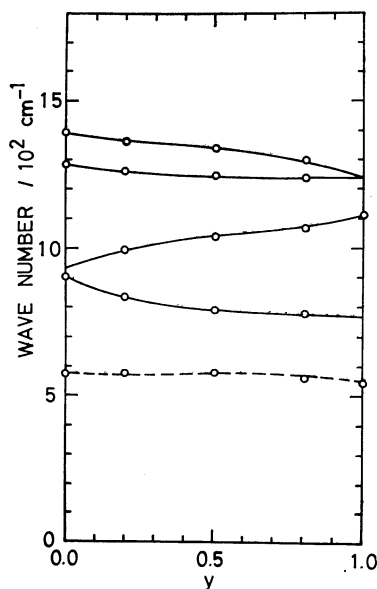


Fig.11. Mode frequencies versus composition, y , of Br_2 doped copolymers $[(\text{C}_2\text{H}_2)_{1-y}(\text{C}_2\text{D}_2)_y]_x$.
—: 300 K,: 160 K.

reveals that this band shifts by about 100 cm^{-1} from 870 cm^{-1} at $y=0$ to 770 cm^{-1} at $y=1.0$ (Fig. 11). However, the frequency shifts of the 1370 cm^{-1} band in the Br_2 doped $(\text{CH})_x$ ($y=0$) and the 1100 cm^{-1} band in the Br_2 doped $(\text{CD})_x$ ($y=1.0$) show quite different behavior. That is, the 1370 cm^{-1} band in $(\text{CH})_x$ and the 1100 cm^{-1} band in $(\text{CD})_x$ shift to lower frequencies with increasing the isotopic substitution. As a result, the 1370 cm^{-1} band in $(\text{CH})_x$ is not correlated directly with the 1100 cm^{-1} band in $(\text{CD})_x$ at any composition y , as is shown in Fig. 11. This fact shows that these complicated spectral patterns should be analysed on the basis of the coupling of the C-H and C-D and C-C vibrations with π -electron transition of low energies occurred with the charged soliton.

The authors would like to thank Mr. Toshiaki Noda and Mr. Gunzo Takamatsu for preparing the Dewar vessel for spectral measurement and the apparatus for the IR absorption measurement.

References

- 1) H. Shirakawa, E. J. Louis, A. G. MacDiarmid, C. K. Chiang, and A. J. Heeger, *J. Chem. Soc., Chem. Commun.*, **1977**, 578.
- 2) C. K. Chiang, M. A. Druy, S. C. Gau, A. J. Heeger, E. J. Louis, A. G. MacDiarmid, Y. W. Park, and H. Shirakawa, *J. Am. Chem. Soc.*, **100**, 1013 (1978).
- 3) C. R. Fincher, Jr., M. Ozaki, M. Tanaka, D. Peebles, L. Lauchlan, A. J. Heeger, and A. G. MacDiarmid, *Phys. Rev. B*, **20**, 1589 (1979).
- 4) M. Tanaka, A. Watanabe, and J. Tanaka, *Bull. Chem. Soc. Jpn.*, **53**, 645 (1980).
- 5) M. Tanaka, A. Watanabe, and J. Tanaka, *Bull. Chem. Soc. Jpn.*, **53**, 3430 (1980).
- 6) M. Tanaka, A. Watanabe, and J. Tanaka, *Chemica Scripta*, **17**, 131 (1981).
- 7) M. Tanaka, H. Fujimoto, and J. Tanaka, *Mol. Cryst. Liq. Cryst.*, **83**, 1107 (1982).
- 8) E. J. Mele and M. J. Rice, *Phys. Rev. B*, **23**, 5397 (1981).
- 9) J. L. Brédas, R. R. Chance, and R. Silbey, *J. Phys. Chem.*, **85**, 756 (1981).
- 10) J. J. Ritsko, *Phys. Rev. Lett.*, **46**, 849 (1981).
- 11) C. R. Fincher, Jr., M. Ozaki, A. J. Heeger, and A. G. MacDiarmid, *Phys. Rev. B*, **19**, 4140 (1979).
- 12) J. F. Rabolt, T. C. Clarke, and G. B. Street, *J. Chem. Phys.*, **71**, 4614 (1979).
- 13) I. Harada, Y. Furukawa, M. Tasumi, H. Shirakawa, and S. Ikeda, *J. Chem. Phys.*, **73**, 4746 (1980).
- 14) B. Francois, M. Bernard, and J. J. Andre, *J. Chem. Phys.*, **75**, 4142 (1981).
- 15) E. J. Mele and M. J. Rice, *Phys. Rev. Lett.*, **45**, 926 (1980).
- 16) E. J. Mele, *Mol. Cryst. Liq. Cryst.*, **77**, 25 (1981).
- 17) S. Etemad, A. Pron, A. J. Heeger, A. G. MacDiarmid, E. J. Mele, and M. J. Rice, *Phys. Rev. B*, **23**, 5137 (1981).
- 18) Y. Furukawa, I. Harada, M. Tasumi, H. Shirakawa, and S. Ikeda, *Chem. Lett.*, **1981**, 1489.
- 19) T. C. Clarke and J. C. Scott, *Solid State Commun.*, **41**, 389 (1982).
- 20) H. Shirakawa and S. Ikeda, *Polym. J.*, **2**, 231 (1971).
- 21) H. G. Lipson and A. Kahan, *Phys. Rev. A*, **133**, 800 (1964).
- 22) W. P. Su, J. R. Schrieffer, and A. J. Heeger, *Phys. Rev. B*, **22**, 2099 (1980).
- 23) E. Burstein, G. Picus, B. Henvi, and R. Wallis, *J. Phys. Chem. Solids*, **1**, 65 (1956).